Control of dissipative tunneling dynamics by continuous wave electromagnetic fields: Localization and large-amplitude coherent motion

Dmitrii E. Makarov and Nancy Makri
School of Chemical Sciences, University of Illinois, 505 South Mathews Avenue, Urbana, Illinois 61801
(Received 19 July 1995)

The dynamics of a dissipative two-level system in a monochromatic field is studied numerically using an iterative path integral scheme that is based on the finite memory range of dissipative influence functionals. The focus of the paper is on the interplay between dissipation and field-induced localization or coherent tunneling. In accord with recent predictions based on approximate treatments, we find that weak dissipation can stabilize the localized state while strong dissipation destroys it. We also demonstrate the possibility of inducing and maintaining large-amplitude coherent oscillations by exploiting the phenomenon of quantum stochastic resonance.

PACS number(s): 05.45.+b, 03.65.−w, 73.20.Dx, 73.40.Gk

I. INTRODUCTION

The possibility of using tailored laser pulses to achieve product selectivity in polyatomic processes has attracted much attention in recent years [1–3]. In order to lead a chemical reaction toward the desired products one must overcome the consequences of intramolecular vibrational energy redistribution. Manipulating charge transfer in nanodevices requires controlling dissipative mechanisms such as electron-phonon interactions [4,5]. In all the above cases, coupling to multidimensional environments is responsible for the inadequacy of simple control schemes.

To date, most theoretical approaches to the problem have been implemented either on small molecules whose dynamics can be extracted by accurate numerical quantum mechanical methods or on dissipative systems via approximate analytical treatments [1–3].

This paper reports the first accurate numerical study of tunneling control in dissipative environments using generic continuous-wave laser fields. For simplicity, we study a symmetric two-level system (TLS) coupled to a harmonic bath and driven by an oscillatory coherent force or by quantum mechanical squeezed light. We assume that a localized state of the TLS has been prepared which might correspond to a hydrogen atom bonded to one of two neighboring atoms during an isomerization reaction or to an excited electron at one site of a double-quantum-well structure. In the absence of driving and for zero system-bath coupling the localized state will execute sinusoidal oscillations between the two equivalent sites. Dissipation generally tends to suppress coherence [6,7] and the dissipative TLS approaches the thermal equilibrium state with equal populations at both sites. The addition of a time-dependent perturbation can change the above picture dramatically, leading under certain dissipationless conditions to destruction of coherent tunneling [8].

In the present study we explore the interplay between driving and dissipation in relation to the TLS dynamics. We are concerned with two questions: First, can the TLS retain its localization for long periods in spite of its coupling to the dissipative environment? Second, can one sustain large-amplitude coherent oscillations? The first question has been the subject of numerous theoretical articles on localization in driven bistable systems [8–17], and we compare our results to these analytical predictions. In a recent Letter [18] we have explored the second question in conjunction with a phenomenon known as stochastic resonance. Here we present a more detailed account of this study.

Central to this work is the development of an iterative path integral scheme for calculating the evolution of the reduced density matrix. Adopting a discretized path integral representation of the propagator and integrating out the harmonic bath leads to a path integral in the TLS space that includes the effects of the dissipative environment through the Feynman-Vernon influence functional which is nonlocal in time [19]. As Monte Carlo integration methods fail due to the oscillatory nature of the integrand, it is hopeless to attempt multidimensional integration in order to obtain long-time dynamics. We have recently shown [20–22] that the nonlocal "memory" terms in the dissipative influence functional decay rapidly as a result of destructive phase interference among a continuum of harmonic bath degrees of freedom. Dropping negligible long-memory terms, one can decompose the multidimensional integral into a series of lower-dimensional integrations. This gives rise to the tensor multiplication scheme which allows iterative propagation over extremely long time periods. In this paper we extend that scheme (which was originally formulated for time-independent Hamiltonians) to include a time-dependent driving term.

Section II describes the tensor multiplication scheme adapted for the case of a time-dependent Hamiltonian. Section III discusses the dissipationless case and the relationship between the current model and that of a TLS coupled to a quantized field. The numerical results for a TLS localized by a strong continuous wave (cw) field and interacting with a dissipative environment are presented in Sec. IV. The conditions that lead to enhancement of coherent motion in the dissipative TLS are described in Sec. V, and Sec. VI concludes.

II. THE TENSOR MULTIPLICATION METHOD

Recently, we proposed [20–22] and applied to a number of problems [18,23] a path integral scheme for propagating the reduced density matrix of a dissipative system in an iterative fashion. This scheme, which uses as a starting point accurate system-specific propagators based on physically motivated reference potentials [24–29], was originally formulated for Hamiltonians without explicit time dependence. The need to treat the problem of a quantum mechanical system interacting with a classical time-dependent electromagnetic field prompted us to extend the method to time-dependent Hamiltonians, a task that will be described in this section.

The Hamiltonian of a symmetric TLS interacting linearly with a bath of harmonic oscillators and with a time-dependent external field is given by

$$H=-\hbar\Omega\sigma_x+\sum_j p_j^2/2m_j+\tfrac{1}{2}m_j\omega_j^2(x_j+c_j\sigma_z/m_j\omega_j^2)^2 + V(t)\sigma_z \;, \quad (1)$$

where $V(t)=V_0\cos(\omega_0 t)$ and σ_x and σ_z are the 2×2 Pauli spin matrices. In the two-state approximation for a particle in a symmetric double-well σ_z is the discrete analogue of the particle coordinate, i.e., $\langle\sigma_z\rangle$ equals 1 (or -1) if the particle is located in the right (or left) well. The population difference between the two eigenstates of the TLS, which are separated by energy $2\hbar\Omega$, is given by $\langle\sigma_x\rangle$. All information about the bath necessary to describe the reduced dynamics of the system is contained in the spectral density function

$$J(\omega)=\frac{\pi}{2}\sum_j\frac{c_j^2}{m_j\omega_j}\delta(\omega-\omega_j) \;. \quad (2)$$

Our aim is to find a numerically tractable representation for the evolution of the reduced density matrix,

$$\tilde{\rho}(t)=\mathrm{Tr}_b\, U(t,0)\rho(0)U^{-1}(t,0) \;, \quad (3)$$

where Tr_b denotes the trace with respect to all bath degrees of freedom and $U(t,0)$ is the time evolution operator that propagates the total wave function through time t. In order to obtain accurate short-time evolution, the Hamiltonian is partitioned into a time-dependent reference system

$$H_0(t)=-\hbar\Omega\sigma_x+V(t)\sigma_z \;, \quad (4)$$

and a time-independent bath Hamiltonian

$$H_{\mathrm{env}}=H-H_0=\sum_j H_j(x_j,p_j,\sigma) \;. \quad (5)$$

Using a symmetric splitting,

$$U(t+\Delta t,t)\approx e^{-iH_{\mathrm{env}}\Delta t/2\hbar}U_0(t+\Delta t,t)e^{-iH_{\mathrm{env}}\Delta t/2\hbar} \;, \quad (6)$$

where $U_0(t+\Delta t,t)$ is the time evolution operator for the reference system, Eq. (4), one obtains the following short-time propagator:

$$\langle\sigma_k\mathbf{x}_k|U(t+\Delta t,t)|\sigma_{k-1}\mathbf{x}_{k-1}\rangle\approx\langle\sigma_k|U_0(t+\Delta t,t)|\sigma_{k-1}\rangle\prod_j\langle x_{j,k}|e^{-iH_j(\sigma_k)\Delta t/2\hbar}e^{-iH_j(\sigma_{k-1})\Delta t/2\hbar}|x_{j,k-1}\rangle \;, \quad (7)$$

where $\sigma_k=\pm1$.

Using the propagator of Eq. (7) and assuming that the system is uncoupled from the bath at $t=0$ so that the initial density matrix is a product of the system and bath density matrices,

$$\rho(0)=\rho_0(0)\rho_b(0) \;, \quad (8)$$

the reduced density matrix can be recast in discretized path integral form

$$\begin{aligned}\tilde{\rho}(\sigma'',\sigma';t)&\equiv\langle\sigma''|\tilde{\rho}(t)|\sigma'\rangle\\ &=\sum_{\sigma_0^+=\pm1}\sum_{\sigma_1^+=\pm1}\cdots\sum_{\sigma_{N-1}^+=\pm1}\sum_{\sigma_0^-=\pm1}\sum_{\sigma_1^-=\pm1}\cdots\sum_{\sigma_{N-1}^-=\pm1}\langle\sigma''|U_0(t,t-\Delta t)|\sigma_{N-1}^+\rangle\cdots\langle\sigma_1^+|U_0(\Delta t,0)|\sigma_0^+\rangle\\ &\quad\times\langle\sigma_0^+|\rho_0(0)|\sigma_0^-\rangle\langle\sigma_0^-|U_0^{-1}(\Delta t,0)|\sigma_1^-\rangle\cdots\langle\sigma_{N-1}^-|U_0^{-1}(t,t-\Delta t)|\sigma'\rangle\\ &\quad\times I(\sigma_0^+,\sigma_1^+,\ldots\sigma_{N-1}^+,\sigma'',\sigma_0^-,\sigma_1^-,\ldots\sigma_{N-1}^-,\sigma';\Delta t) \;. \end{aligned}\quad (9)$$

Here the superscripts $\pm$ refer to the forward and backward paths that evolve in the positive and negative time directions and, if the harmonic oscillator bath has started out in thermal equilibrium, its influence functional is generally of the form

$$I=\exp\left\{-\frac{1}{\hbar}\sum_{k=0}^{N}\sum_{k'=0}^{k}(\sigma_k^+-\sigma_k^-)(\eta_{kk'}\sigma_{k'}^+-\eta_{kk'}^*\sigma_{k'}^-)\right\} \;, \quad (10)$$

where $\sigma_N^+=\sigma''$ and $\sigma_N^-=\sigma'$ and the temperature-dependent coefficients $\eta_{kk'}$ have been given in [21] in terms of the spectral density.

The tensor multiplication scheme formulated in [20] is based on the observation that the coefficients $\eta_{kk'}$, which represent a discrete analogue of the bath response function [30], fall off rapidly as $|k-k'|$ is increased. In other words, the bath-induced memory has finite range, leading to decay of long-time interactions in the influence functional. Neglecting all $\eta_{kk'}$ corresponding to $|k-k'|$ greater than some $\Delta k_{\max}$ enables one to represent Eq. (9) as a $\Delta k_{\max}$th order iterative tensor multiplication [31]. Representing the variables $\{\sigma_k^\pm\}$ collectively as a four-dimensional array (vector), the scheme consists of the following steps [22].

(1) Define a *propagator tensor* Λ of rank $\Delta k_{\max}+1$ as

$$\Lambda^{(\Delta k_{\max}+1)}(\sigma_k^\pm,\sigma_{k+1}^\pm,\ldots,\sigma_{k+\Delta k_{\max}}^\pm;(k+1)\Delta t,k\Delta t)=K(\sigma_k^\pm,\sigma_{k+1}^\pm;(k+1)\Delta t,k\Delta t)I_0(\sigma_k^\pm)I_1(\sigma_k^\pm,\sigma_{k+1}^\pm)\times I_2(\sigma_k^\pm,\sigma_{k+2}^\pm)\cdots I_{\Delta k_{\max}}(\sigma_k^\pm,\sigma_{k+\Delta k_{\max}}^\pm)\,, \tag{11}$$

where

$$I_0(\sigma_k^\pm)=\exp\left\{-\frac{1}{\hbar}(\sigma_k^+-\sigma_k^-)(\eta_{kk}\sigma_k^+-\eta_{kk}^*\sigma_k^-)\right\}, \tag{12}$$

$$I_{\Delta k}(\sigma_k^\pm,\sigma_{k+\Delta k}^\pm)=\exp\left\{-\frac{1}{\hbar}(\sigma_{k+\Delta k}^+-\sigma_{k+\Delta k}^-)\times(\eta_{k+\Delta k,k}\sigma_k^+-\eta_{k+\Delta k,k}^*\sigma_k^-)\right\},\quad \Delta k\geq 1\,. \tag{13}$$

The matrix $K(\sigma_k^\pm,\sigma_{k+1}^\pm;(k+1)\Delta t,k\Delta t)$ propagates the density matrix of the time-dependent system, Eq. (4), through time increment Δt), i.e.,

$$\rho_0(\sigma_{k+1}^\pm(k+1)\Delta t)=\sum_{\sigma_k^\pm}K(\sigma_k^\pm,\sigma_{k+1}^\pm;(k+1)\Delta t,k\Delta t)\times\rho_0(\sigma_k^\pm;k\Delta t)\,, \tag{14}$$

and is equal to

$$K(\sigma_k^\pm,\sigma_{k+1}^\pm;(k+1)\Delta t,k\Delta t)=\langle\sigma_{k+1}^+|U_0((k+1)\Delta t,k\Delta t)|\sigma_k^+\rangle\times\langle\sigma_k^-|U_0^{-1}((k+1)\Delta t,k\Delta t)|\sigma_{k+1}^-\rangle\,. \tag{15}$$

The system propagators are calculated by solving numerically the Schrödinger equation

$$i\hbar\dot{U}_0(t,t_0)=H_0(t)U_0(t,t_0)\,, \tag{16}$$

subject to the "initial condition"

$$\langle\sigma'|U_0(t_0,t_0)|\sigma\rangle=\delta_{\sigma'\sigma}\,.$$

(2) Define the *reduced density tensor* $\mathbf{A}^{(\Delta k_{\max})}$ with the following initial condition

$$A^{(\Delta k_{\max})}(\sigma_0^\pm,\sigma_1^\pm,\ldots,\sigma_{\Delta k_{\max}-1}^\pm;0)=\langle\sigma_0^+|\rho_0(0)|\sigma_0^-\rangle\,. \tag{17}$$

(3) Propagate $\mathbf{A}^{(\Delta k_{\max})}$ through time Δt according to the relation

$$A^{(\Delta k_{\max})}(\sigma_{k+1}^\pm,\ldots,\sigma_{k+\Delta k_{\max}}^\pm;(k+1)\Delta t)=\sum_{\sigma_k^\pm=\pm1}\Lambda^{(\Delta k_{\max}+1)}(\sigma_k^\pm,\ldots,\sigma_{k+\Delta k_{\max}}^\pm;(k+1)\Delta t,k\Delta t)\times A^{(\Delta k_{\max})}(\sigma_k^\pm,\ldots,\sigma_{k+\Delta k_{\max}-1}^\pm;k\Delta t)\,. \tag{18}$$

(4) Finally, project out the auxiliary dimensions in the tensor $\mathbf{A}^{(\Delta k_{\max})}$ to obtain the reduced density matrix at time $N\Delta t$

$$\tilde{\rho}(\sigma_N^\pm;N\Delta t)=A^{(\Delta k_{\max})}(\sigma_N^\pm,\sigma_{N+1}^\pm=\cdots=\sigma_{N+\Delta k_{\max}-1}^\pm=0;N\Delta t)I_0(\sigma_N^\pm)\,. \tag{19}$$

III. ZERO DISSIPATION: FLOQUET PICTURE OF THE DYNAMICS AND QUANTUM-CLASSICAL CORRESPONDENCE

A. The Floquet theorem

Before proceeding to the study of dissipative driven systems, it is helpful to introduce the Floquet formalism for the dynamics of periodically driven quantum systems.

The Floquet theorem [32] asserts that if the Hamiltonian of a system is periodic in time with period τ, $H_0(t)=H_0(t+\tau)$, then there are solutions to the Schrödinger equation,

$$i\hbar\dot{\phi}_n(t)=H_0(t)\phi_n(t) , \tag{20}$$

that are eigenfunctions of the Floquet operator $F\equiv U_0(t+\tau,t)$, i.e.,

$$\phi_n(t+\tau)=e^{-i\varepsilon_n\tau/\hbar}\phi_n(t) . \tag{21}$$

This theorem reflects the fact that the time-translation operator for propagation by multiples of the period τ commutes with the Hamiltonian. The states ϕ_n are the Floquet states and the quantities ε_n are the quasienergies. Apparently, if ε_n is a quasienergy, then the family of quasienergies $\varepsilon_n+k\hbar\omega$ (where k is an integer) corresponds to the same physical state. A way to uniquely define the quasienergy is to require that it approach continuously the energy eigenvalue of the system as the time-dependent part of the Hamiltonian vanishes. The quasienergies play the role of energies in the stroboscopic picture of the dynamics: as long as the time is only allowed to be a multiple of τ, the time evolution of the Floquet states is the same as that of energy eigenstates for a time-independent Hamiltonian.

B. Quantum-classical correspondence and localization

A classical harmonic oscillator with frequency ω_0 and mass μ large enough for it not to be affected by the coupled quantum mechanical subsystem will produce the same response as the periodic field $V(t)=V_0\cos(\omega_0 t)$. On the other hand, a fully quantum mechanical version of the model can be studied [33,17], with the Hamiltonian,

$$H=-\hbar\Omega\sigma_x+CQ\sigma_z+\frac{P^2}{2\mu}+\frac{1}{2}\mu\omega_0^2Q^2+H_{\text{env}} , \tag{22}$$

which should in the classical limit reproduce the effect of the classical periodic field. The Hamiltonian of this type describes, e.g., a two-level atom in a resonator cavity [33].

The Hamiltonian (22) represents two coupled parabolic surfaces, $V_{1,2}(Q)=\mu\omega_0^2(Q\pm C/\mu\omega_0^2)^2/2-C^2/2\mu\omega_0^2$ which intersect at $Q=0$. In the absence of tunneling ($\Omega=0$) each energy level of the harmonic oscillator $E_n=\hbar\omega_0(n+1/2)$ would be doubly degenerate. Tunneling in general lifts this degeneracy and splits each energy level into a doublet. If a level turns out to be degenerate, then the system once prepared on one of the surfaces will never reach the other.

In the semiclassical approximation for the oscillator one finds [17] that the splitting Δ_n of the nth doublet is equal to the quasienergy splitting of the classically driven TLS with the field amplitude given by

$$\tfrac{1}{2}\mu\omega_0^2V_0^2=C^2\hbar\omega_0(n+1/2) . \tag{23}$$

On the other hand, the splitting can be evaluated quantum mechanically using nearly degenerate perturbation theory

$$\begin{aligned}\Delta_n&=\Delta_0\int dQ\,\psi_n(Q+C/\mu\omega_0^2)\psi_n(Q-C/\mu\omega_0^2)\\&=\exp(-a/2)L_n(a) ,\end{aligned} \tag{24}$$

where $\Delta_0=2\hbar\Omega$, $a=2C^2/\hbar\mu\omega_0^3$, ψ_n are harmonic oscillator eigenstates with frequency ω_0, and L_n is the nth Laguerre polynomial. In the limit $n\gg1$ zeros of the Laguerre polynomial a_j are related to the zeros of the Bessel function $J_0(z)$ by [34]

$$a_j=z_j^2/(4n+2) .$$

Using Eqs. (23) and (24) one obtains the localization condition in the form

$$2V_0/\hbar\omega_0=z_j , \tag{25}$$

which is the standard result for the classically driven TLS [8–10]. The quantized version of the model is very instructive and will be extensively discussed in Sec. IV to describe the effect of dissipation on laser-induced localization.

IV. LOCALIZATION VERSUS DISSIPATION

Grossman *et al.* [35] and Dittrich, Oeschlägel, and Hänggi [36] have shown, based on approximate treatments such as a master equation approach and stochastic differential equations, that under certain conditions dissipation should stabilize a nearly localized state rather than destroy it. Such stabilization is also observed for the model of a TLS coupled to a single cavity mode [17,33] and a macroscopic environment with continuous spectrum: As explained in Sec. III B, the spectrum of the system consists of tunneling doublets spaced by the vibrational quantum of the cavity mode $\hbar\omega_0$. If there is an upper cutoff $\omega_c<\omega_0$ for the bath spectral density such that $J(\omega)$ vanishes if $\omega>\omega_c$, then phonon-induced transitions between different doublets are prohibited in low orders of perturbation theory. Therefore, once the system is prepared in a single doublet Δ_n, its dynamics is well described by an effective Hamiltonian $H_{\text{eff}}=-(\Delta_n/2)\sigma_x$, which enables one to use the elaborate theory of the dissipative TLS [6,7].

Based on quantum-classical correspondence, the same dynamics should follow from the time-dependent Hamiltonian of Eq. (1) after one replaces $H_0(t)$ by a TLS Hamiltonian of the form $H_{\text{eff}}=-(\Delta\varepsilon/2)\sigma_x$, where $\Delta\varepsilon$ is the quasienergy splitting of the driven TLS. Such a replacement is superficially similar to the well known rotating wave approximation [37], which also reduces the time-dependent problem to a time-independent one, and can be justified only in the vicinity of the localization point where the quasienergy splitting is small.

For concreteness, consider the case of the Ohmic spectral density with exponential cutoff,

$$J(\omega)=(\pi\hbar\alpha/2)\omega\exp(-\omega/\omega_c) . \tag{26}$$

For temperatures not too low but such that $k_BT<\hbar\omega_c$, the TLS relaxes to the equilibrium state with a rate given by [6,7]

$$k=(\Delta\varepsilon^2/\hbar^2\omega_c)\frac{\pi^{1/2}}{2}\frac{\Gamma(\alpha)}{\Gamma(\alpha+1/2)}(\pi k_B T/\hbar\omega_c)^{2\alpha-1} , \quad (27)$$

whence the incoherent tunneling rate decreases with increasing temperature if the Kondo parameter α is less than $\frac{1}{2}$.

An important conclusion is that the *stationary state* of the driven two-level system is, to a good accuracy, the thermodynamic equilibrium state of a time-independent TLS with an appropriate splitting, leading to the possibility of manipulating this equilibrium by changing the field [38]. The same picture emerges from Dakhnovskii's analysis of the noninteracting blip approximation for the dynamics of a driven TLS [39]. However, this picture entails a time-independent equilibrium state of the two-level system. Dakhnovskii [39] argued that the time-dependent corrections to the equilibrium state should be small in the case of strong dissipation and/or near the localization point; otherwise this simple picture is invalidated by time-dependent contributions to the density matrix in the steady state. No matter how small, these are responsible for the delocalization in the case where the quasienergy splitting is exactly zero and the system is localized in the absence of coupling to the environment: Indeed, viewing coupling to the bath as random noise, it

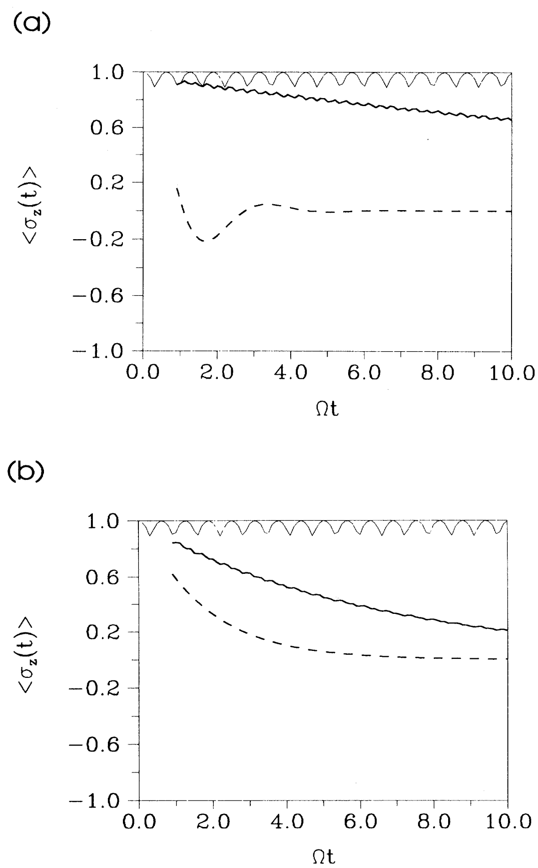

FIG. 1. The expectation value $\langle\sigma_z(t)\rangle$ plotted as a function of Ωt for a symmetric TLS driven by a monochromatic field with frequency $\omega_0=10.0\Omega$ and amplitude $V_0=11.965\,75\hbar\Omega$. The cutoff frequency is $\omega_c=7.5\Omega$. The Kondo parameter is $\alpha=0.16$, the temperature is (a) $k_B T=2\hbar\Omega$ and (b) $k_B T=20\hbar\Omega$. Dashed line: field-free dynamics ($V_0=0$). Thin solid line: dissipationless case ($\alpha=0$).

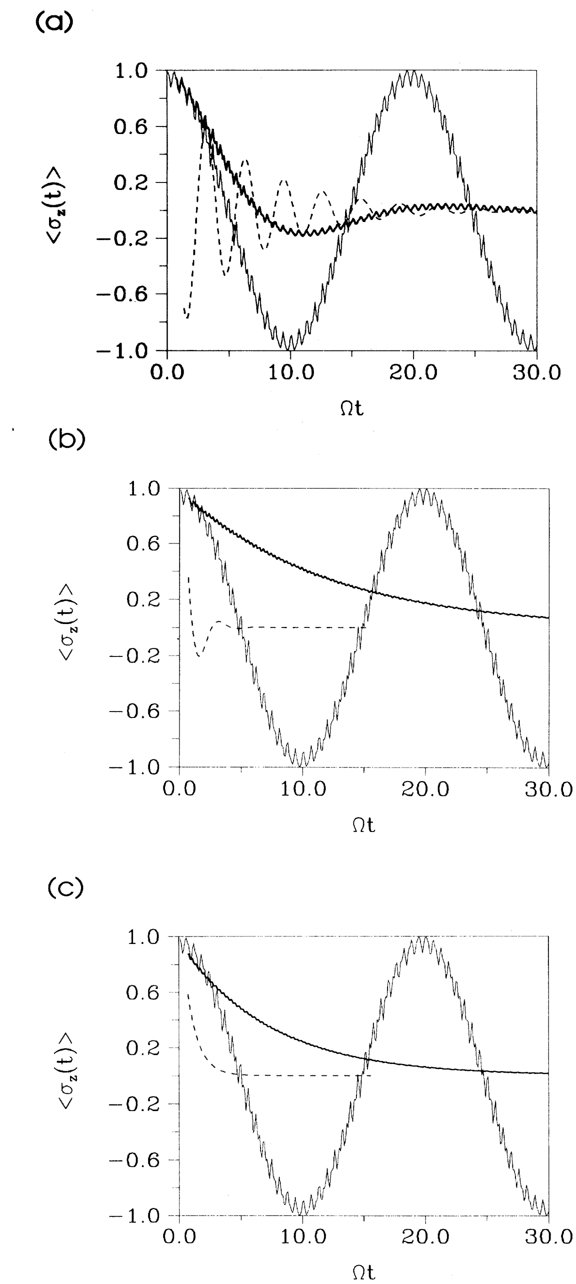

FIG. 2. The expectation value $\langle\sigma_z(t)\rangle$ plotted as a function of Ωt for a symmetric TLS driven by a monochromatic field with frequency $\omega_0=10.0\Omega$ and amplitude $V_0=10.5\hbar\Omega$. The cutoff frequency is $\omega_c=7.5\Omega$. The Kondo parameter is $\alpha=0.04$, the temperature is (a) $k_B T=1.333\hbar\Omega$, (b) $k_B T=10\hbar\Omega$, and (c) $k_B T=40\hbar\Omega$. Dashed line: field-free dynamics ($V_0=0$). Thin solid line: dissipationless case ($\alpha=0$).

is natural to expect that such noise should destroy phase coherence that is clearly necessary to maintain the localized state [14,15]. Therefore, any localized state should eventually be destroyed, unless there is a spontaneous symmetry breaking effect produced by the dissipative environment itself.

These two antagonistic tendencies, stabilization of the localized state and delocalization, have been observed in numerical studies of the driven dissipative double well [35,36], where dissipation was taken into account by means of a random force component in the Hamiltonian or by using master equation techniques. In a double well another mechanism of destruction of the localized state is also possible [17], which involves transitions to upper doublets of the double well where the localization criterion of Eq. (25) does not hold. Our present analysis is done on the simpler model of a two-level system and is not concerned with such a mechanism.

Our numerical results presented in Figs. 1 and 2 confirm that weak dissipation stabilizes a nearly localized state while strong dissipation tends to destroy localization. Figure 1 displays the average position of the TLS driven by a classical field of frequency $\omega_0 = 10\Omega$ and amplitude $V_0 = 11.965\,75\hbar\Omega$. In the initial state the position is taken to be $\langle \sigma_z(0) \rangle = 1$. In the absence of dissipation, these parameters correspond to exact localization at times which are multiples of the period. With finite values of the Kondo parameter, Fig. 1 shows that $\langle \sigma_z(t) \rangle$ decays with slope which increases with temperature. It is also seen that localization of the driven TLS is destroyed more slowly than in the field-free case. In Fig. 2 a driving field of the same frequency is used, but the field amplitude $V_0 = 10.5\hbar\Omega$ is now shifted slightly away from the localization condition. The average position $\langle \sigma_z(t) \rangle$ is shown in Fig. 2 at three different temperatures. It is seen that weak dissipation can aid localization rather than destroying it, in accord with the observations made in [35,36]. Here the temperature dependence of the delocalization rate in the dissipative TLS is not monotonic: At low temperatures, $\langle \sigma_z(t) \rangle$ decays more slowly than in the dissipationless case, in agreement with the result of Refs. [35,36]. Modest increase of temperature leads to further stabilization of the localized state, while faster decay toward equilibrium is observed at high temperatures. As seen in Fig. 3, these effects arise from (nearly) periodic fluctuations in the TLS eigenstate populations induced by the interplay between the driving field and dissipation.

The effects of a quantum mechanical picture of the radiation, where the field is in an eigenstate of the number operator, are explored in Fig. 4. This figure shows the dissipative dynamics of a TLS coupled to a *quantum* oscillator, Eq. (22), in the state with quantum number $n = 1$. As described in Sec. III B, the parameters of the quantum oscillator were chosen to correspond to those of the classical field of Fig. 2. However, because the quantum number n is low and the semiclassical theory for the quasienergies [17] is not accurate in this regime, the coupling C had to be slightly adjusted from that given by Eq. (23) in order to provide the energy splitting of the $n = 1$ doublet exactly equal to the quasienergy splitting in the classical field and thus to produce the same oscillation period in the absence of dissipation. The value of C needed for this is such that the value of V_0 that follows then from Eq. (23) is $10.655\hbar\Omega$ rather than the classical field amplitude $10.5\hbar\Omega$. Apart from the small ω_0-periodic fluctuations in the classical case of Fig. 2, the dissipation-free dynamics is identical for the classical and quantum fields. As in the case of classical driving, for moderately high temperatures $\hbar\Delta/k_B T = 0.1$, dissipation results in incoherent relaxation with a rate that decreases as the temperature is increased, while at higher temperatures ($\hbar\Delta/k_B T = 0.025$) the relaxation rate increases with the temperature. This destruction of localization is

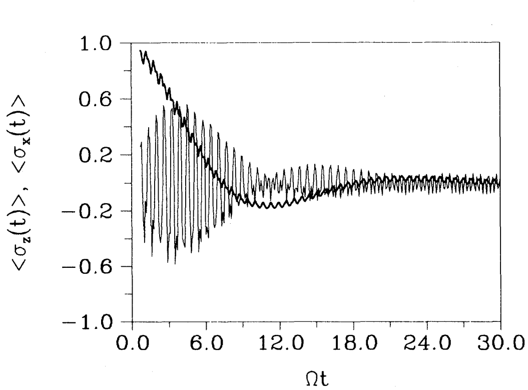

FIG. 3. The expectation values $\langle \sigma_z(t) \rangle$ (heavy solid line) and $\langle \sigma_x(t) \rangle$ (thin solid line) plotted as functions of Ωt for a symmetric TLS driven by a monochromatic field with frequency $\omega_0 = 10.0\Omega$ and amplitude $V_0 = 10.5\hbar\Omega$. The cutoff frequency is $\omega_c = 7.5\Omega$. The Kondo parameter is $\alpha = 0.04$, the temperature $k_B T = 1.333\hbar\Omega$.

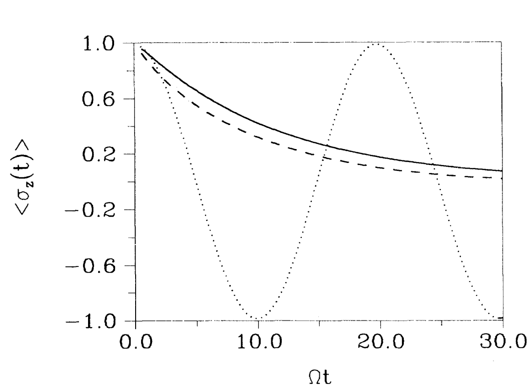

FIG. 4. The expectation value $\langle \sigma_z(t) \rangle$ plotted as a function of Ωt for a symmetric TLS coupled to a quantum cavity field Eq. (22) in the first excited state at temperature $k_B T = 10\hbar\Omega$ (solid line) and $k_B T = 40\hbar\Omega$ (dashed line). The bath parameters are the same as in Fig. 2, see text for the other parameters. Dashed line: dissipationless case.

caused by the bath-induced transitions among different doublets of the harmonic oscillator coupled to the TLS, which invalidate the independent doublet picture discussed in Sec. II B.

V. LARGE-AMPLITUDE COHERENT OSCILLATIONS

As we have seen in Sec. IV, strong periodic fields tend to suppress periodic oscillations of the particle in the long-time limit. An interesting question is whether one can induce large-amplitude tunneling oscillations by a suitable monochromatic field. In a recent letter [18], we argued that this is possible with a field that is tuned near resonance with the transition between the two eigenstates of the TLS $\omega_0 \approx 2\Omega$. Here we present a more detailed account of the theory and more numerical calculations showing a strongly nonlinear response to the periodic force in this regime.

Figure 5 presents an example of large-amplitude coherent oscillations obtained with the resonant field $V_0=0.5\hbar\Omega$. The dependence of the oscillation amplitude on the Kondo parameter α is explored in Fig. 6, demonstrating a pronounced maximum. The value of α where the maximum occurs is proportional to V_0. Such a peak is known from classical studies [40,41] as a "stochastic resonance," a phenomenon where the response of a nonlinear system to the external periodic force is enhanced by noise. Such a phenomenon has also been predicted for a quantum overdamped asymmetric bistable system [42]. For the cases of high- and low-frequency driving, a variety of nonlinear effects in the steady-state dynamics of a dissipative TLS have been studied analytically, based on the noninteracting blip approximation [43,44].

The case where the field frequency is comparable to the TLS frequency is more difficult to handle analytically. If the system-bath coupling is weak, though, one might hope that the traditional optical Bloch equations, which treat the driving field in the rotating wave approximation, will produce a meaningful result. Specifically, these equations read (see, e.g., [37])

$$\langle \dot{\tilde{\sigma}}_x \rangle = -(V_0/\hbar)\langle \tilde{\sigma}_y \rangle - (1/\tau_1)(\langle \tilde{\sigma}_x \rangle - \langle \sigma_x^{\rm eq} \rangle) ,$$

$$\langle \dot{\tilde{\sigma}}_y \rangle = (2\Omega-\omega_0)\langle \tilde{\sigma}_z \rangle - (1/\tau_2)\langle \tilde{\sigma}_y \rangle + (V_0/\hbar)\langle \tilde{\sigma}_x \rangle ,$$

$$\langle \dot{\tilde{\sigma}}_x \rangle = -(2\Omega-\omega_0)\langle \tilde{\sigma}_y \rangle - (1/\tau_2)\langle \tilde{\sigma}_z \rangle \quad (28)$$

where the tilde indicates the rotating-frame representation in which the Pauli operators are given by

$$\tilde{\sigma}_z = \sigma_x \cos(\omega_0 t) + \sigma_y \sin(\omega_0 t) ,$$

$$\tilde{\sigma}_y = \sigma_y \cos(\omega_0 t) - \sigma_z \sin(\omega_0 t) ,$$

$$\tilde{\sigma}_x = \sigma_x .$$

The population relaxation and dephasing times [45] τ_1 and τ_2, respectively, are given by

$$\tau_1^{-1} = 2\hbar^{-1} J(2\Omega)\coth(\hbar\Omega/k_B T) \quad (29)$$

and for the present model $\tau_2 = 2\tau_1$. Finally,

$$\langle \sigma_x^{\rm eq} \rangle = \tanh(\hbar\Omega/k_B T) \quad (30)$$

is the equilibrium value of $\langle \sigma_x \rangle$ in the absence of the field.

Solving Eqs. (28) for the limiting steady-state expectation values of the Pauli operators and transforming back to the original reference frame one obtains

$$\langle \sigma_x \rangle_{\rm lim} = \langle \tilde{\sigma}_x \rangle_{\rm lim} = \tanh(\hbar\Omega/k_B T) \left[1 + \frac{V_0^2 \tau_1 \tau_2/\hbar^2}{1+\tau_2^2(2\Omega-\omega)^2} \right]^{-1} , \quad (31)$$

and the maximum steady-state oscillation amplitude of $\langle \sigma_z \rangle$ (which corresponds to $\langle \sigma_y \rangle = 0$)

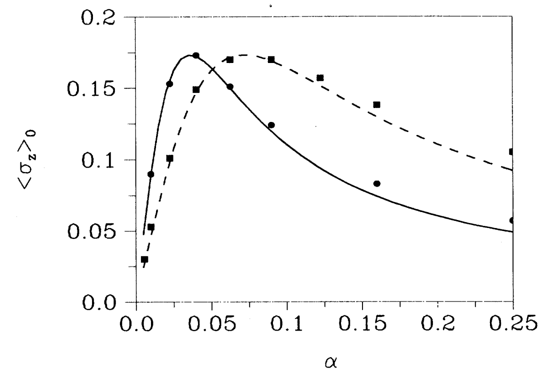

FIG. 6. Steady-state oscillation amplitude $\langle \sigma_z \rangle_0$ plotted as a function of the Kondo parameter for $\omega_0=2\Omega$, $V_0=0.5\hbar\Omega$ [circles: simulation data, solid line: Eq. (36)], and $V_0=\hbar\Omega$ [squares: simulation data, dashed line: Eq. (36)]. The temperature is $k_B T=4.0\hbar\Omega$, the bath cutoff frequency $\omega_c=7.5\Omega$.

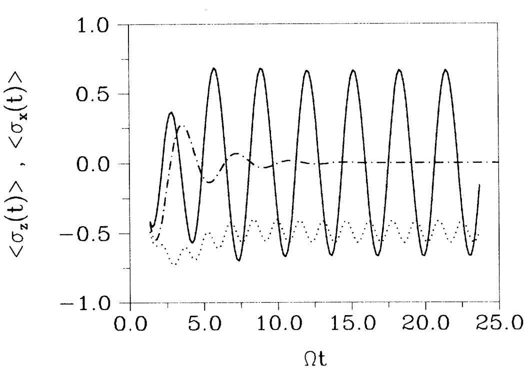

FIG. 5. The expectation values $\langle \sigma_z(t) \rangle$ (solid line) and $\langle \sigma_x(t) \rangle$ (dotted line) plotted as functions of Ωt for a symmetric TLS driven by a monochromatic field with frequency $\omega_0=2\Omega$ and amplitude $V_0=0.5\hbar\Omega$ at temperature $k_B T=0.278\hbar\Omega$. The bath cutoff frequency is $\omega_c=7.5\Omega$, the Kondo parameter $\alpha=0.16$. Chain-dotted line: field-free dynamics ($V_0=0$).

$$\langle \sigma_z \rangle_0 = (\langle \tilde{\sigma}_z \rangle^2_{\lim} + \langle \tilde{\sigma}_y \rangle^2_{\lim})^{1/2} , \\ = \frac{V_0 \tau_2 [1+(\omega_0 - 2\Omega)^2 \tau_2^2]^{1/2}/\hbar}{1+V_0^2 \tau_1 \tau_2/\hbar^2 + (\omega_0 - 2\Omega)^2 \tau_2^2} \tanh(\hbar\Omega/k_B T) . \quad (32)$$

Here the subscript "lim" denotes constant steady-state values of the Pauli operators in the rotating frame and $\langle \sigma_z \rangle_0$ is the steady-state oscillation amplitude of $\langle \sigma_z(t) \rangle$, and is given in the rotating-frame picture by the projection of the expectation value of the Pauli spin operator onto the *yz* plane.

Recently, it has been shown [46] that Eqs. (28) are only valid in the weak field limit and are to be modified for strong fields. The generalized Bloch equations obtained in Ref. [46] are different from Eqs. (28) in that the relaxation times τ_1 and τ_2 are field-dependent and also cross relaxation terms are present. The validity of the rotating-wave approximation itself becomes questionable away from the resonance conditions. For these reasons Eq. (32) yields an incorrect result in the limit of low-frequency driving $\omega_0 \to 0$. Indeed, for small V_0 one expects in this limit that the two-level system will follow adiabatically the external field, resulting in a value of $\langle \sigma_z \rangle_0$ which is independent of τ_1 and τ_2. Instead, Eq. (32) predicts that the oscillation amplitude $\langle \sigma_z \rangle_0$ will depend on τ_2 and vanish in the limit of short dephasing times.

The analysis that follows avoids use of the rotating-wave approximation and, as will be shown below, produces meaningful results in the parameter range studied numerically, as well as in the limit of low or high driving frequency: We define an instantaneous energy bias of the TLS due to both the driving field and the bath oscillators as $f(t) = V_0 \cos(\omega_{0t}) + \sum_j c_j x_j(t)$. Then the Heisenberg equations of motion for the evolution of the Pauli matrices are

$$\dot{\sigma}_x(t) = -2\sigma_y(t) f(t)/\hbar , \\ \dot{\sigma}_y(t) = 2\Omega \sigma_z(t) + 2\sigma_x(t) f(t)/\hbar , \\ \dot{\sigma}_z(t) = -2\Omega \sigma_y(t) , \quad (33)$$

whence $\langle \sigma_z \rangle$ obeys the equation

$$\langle \ddot{\sigma}_z \rangle + 2(\Omega)^2 \langle \sigma_z \rangle = -4\Omega \langle \sigma_x \rangle (V_0/\hbar) \cos(\omega t) \\ -4(\Omega/\hbar) \sum_j c_j \langle \sigma_x x_j(t) \rangle . \quad (34)$$

Next we use the weak coupling approximations formulated by Dekker [47], which enable one to convert the last term in Eq. (34) to a damping term and further treat it in the Markovian approximation. In doing so, the bath is treated as causing stochastic energy bias fluctuations that are unaffected by the dynamics of the TLS itself. As a result, a harmonic oscillator equation is obtained with the periodic force proportional to the population difference $\langle \sigma_x \rangle$ between the two eigenstates of the TLS

$$\langle \ddot{\sigma}_x \rangle + (2\Omega)^2 \langle \sigma_z \rangle + (2/\tau_2) \langle \dot{\sigma}_z \rangle = -4\Omega \langle \sigma_x \rangle \\ \times (V_0/\hbar) \cos(\omega_0 t) . \quad (35)$$

To obtain an approximate solution to Eq. (35), we use the fact that the population difference between the TLS eigenstates $\langle \sigma_x \rangle$ stays practically constant in the steady state, as shown in Fig. 5. This observation suggests using the steady-state value Eq. (31) obtained from the rotating-wave approximation. Note that for V_0 small enough, Eq. (31) gives the correct answer in the limit of high or low driving frequency, as well as for resonant pumping.

With the approximation of Eq. (31), Eq. (35) is the standard equation of motion for a forced harmonic oscillator with dissipation. The steady-state solution oscillates with the amplitude

$$\langle \sigma_x \rangle_0 = \frac{4\Omega V_0}{\hbar[(\omega_0^2 - 4\Omega^2)^2 + \omega_0^2/\tau_1^2]^{1/2}} \langle \sigma_x \rangle_{\lim} . \quad (36)$$

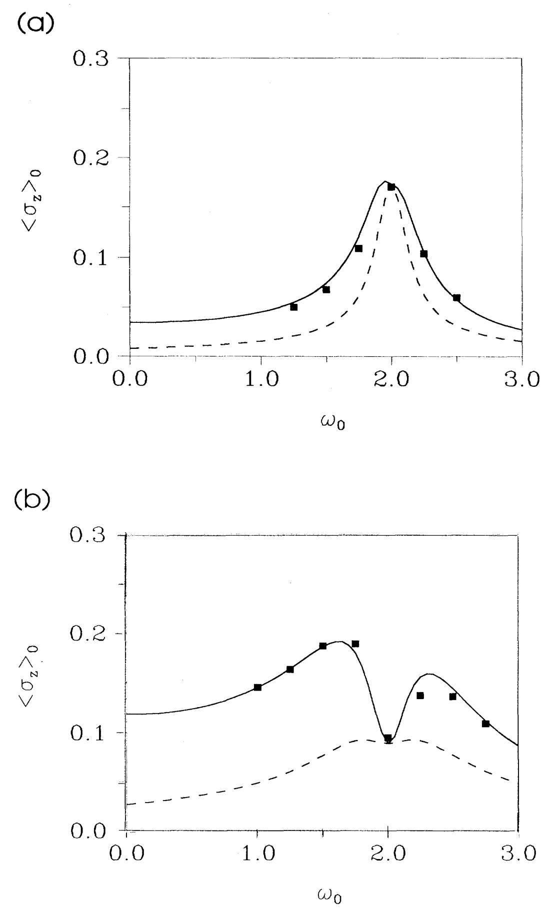

FIG. 7. Steady-state oscillation amplitude $\langle \sigma_z \rangle_0$ plotted as a function of the driving field frequency ω_0 for the field amplitude V_0 equal to (a) $0.14\hbar\Omega$ and (b) $0.5\hbar\Omega$. The temperature is $k_B T = 4.0\hbar\Omega$, the Kondo parameter $\alpha = 0.01$, the bath cutoff frequency $\omega_c = 7.5\Omega$. Squares: simulation data, solid line: Eq. (36), dashed line: Eq. (32).

Comparing Eqs. (32) and (36), both give identical results at resonance $\omega_0=2\Omega$. The theory is in good agreement with our numerical data, as indicated in Fig. 5. For resonant pumping, the maximum oscillation amplitude is achieved if the field amplitude takes an optimal value of

$$V_0^{\text{opt}}=\hbar(\tau_1\tau_2)^{-1/2} \tag{37}$$

and is equal to

$$\langle\sigma_z\rangle_0^{\max}=(\tau_1/\tau_2)^{1/2}\tanh(\hbar\Omega/k_BT)\ ,$$

which is independent of the coupling to the bath for the current model where $\tau_2=2\tau_1$. For a fixed field intensity, the theory predicts a stochastic resonance as a function of the relaxation time, in accord with the numerical data.

Away from the resonant condition $\omega_0=2\Omega$, the results predicted by Eqs. (32) and (36) are different. While Eq. (36) gives the correct low-frequency (static) limit for small V_0, Eq. (32) does not. Further, for a high-frequency field Eq. (32) predicts that the oscillation amplitude will be inversely proportional to ω_0 while Eq. (36) yields a ω_0^{-2} dependence. The frequency dependences given by Eqs. (32) and (36) are compared with the numerical data in Fig. 7, demonstrating that our theory provides an accurate quantitative description of the response of the TLS to an external periodic force throughout the entire frequency range while the result given by the optical Bloch equations is correct only for the resonant field.

In contrast with the rotating-wave approximation, our data indicate that large-amplitude oscillations can be achieved even with an appropriate off-resonant field, as shown in Fig. 7(b) where the oscillation amplitude exhibits two pronounced off-resonant peaks of approximately the same magnitude as the single peak [Fig. 7(a)] obtained for a weaker driving field $V_0\approx V_0^{\text{opt}}$.

VI. CONCLUDING REMARKS

In this paper we have systematically investigated the dynamics of dissipative two-level systems in the regime of strongly nonlinear response to the driving field. To be in this regime, the field need not be very strong on the energy scale of the TLS; in fact, as shown in Sec. V, linear response is violated at fields arbitrarily weak as long as the coupling to the dissipative environment is weak enough.

We have confirmed numerically the finding of Refs. [35,36] that the localized effect of *strong fields* ($V_0>\hbar\Omega$) can be stabilized by weak dissipation in a certain temperature range. In this range the effect of a quantized cavity field [33] is similar to that of a classical field, suggesting a simple picture of the dynamics based on an effective time-independent TLS [17].

The possibility of inducing and sustaining coherent oscillations whose amplitude is not significantly suppressed by dissipative effects is another important conclusion, which suggests ways of overcoming the consequences of intramolecular vibrational energy redistribution in various laser control schemes [1–3]. This effect can be accomplished with a weak optimum field proportional to the relaxation rate, as opposed to mode-locking approaches [48] that yield the best results if the driving field is strong. A different method of inducing large-amplitude charge oscillations in an asymmetric electron-transfer system with strong field pulses has recently been proposed in [49], based on the idea that a strong driving field may affect the equilibrium of the TLS.

From a technical point of view, we have demonstrated that the tensor multiplication scheme [20–22] is well suited to describing the long-time dynamics of laser-driven systems and thus succeeds in exploring the nature of the steady state of a strongly nonequilibrium driven nonlinear system, a task that other numerical methods have so far failed to accomplish. Potential applications of this approach are abundant, from calculation of absorption line shapes to the dynamics of charge transfer in semiconductor heterostructures. We intend to pursue these applications in our future work.

ACKNOWLEDGMENTS

This work has been supported by the Arnold and Mabel Beckman Foundation and the National Science Foundation through Grant No. NSF CHE 93-13603.

[1] P. Brumer and M. Shapiro, Annu. Rev. Phys. Chem. **43**, 257 (1992).
[2] W. S. Warren, H. Rabitz, and M. Dahleh, Science **259**, 1581 (1993).
[3] *Mode Selective Chemistry,* edited by J. Jortner, R. D. Levine, and B. Pullman (Dordrecht, Boston, 1991).
[4] M. S. C. Luo, S. L. Chuang, P. C. M. Planken, I. Brener, and M. Nuss, Phys. Rev. B **48**, 4903 (1993); **48**, 11 043 (1993).
[5] I. Brener, P. C. M. Planken, M. C. Nuss, L. Pfeiffer, D. E. Leaird, and A. M. Weiner, Appl. Phys. Lett. **63**, 2213 (1993).
[6] A. J. Leggett, S. Chakravarty, A. T. Dorsey, M. P. A. Fisher, A. Garg, and M. Zwerger, Rev. Mod. Phys. **59**, 1 (1987).
[7] U. Weiss, *Quantum Dissipative Systems* (World Scientific, Singapore, 1993).
[8] F. Grossmann, T. Dittrich, P. Jung, and P. Hänggi, Phys. Rev. Lett. **67**, 516 (1991).
[9] F. Grossmann and P. Hänggi, Europhys. Lett. **18**, 571 (1992).
[10] J. M. Gomez Llorente and J. Plata, Phys. Rev. A **45**, R6958 (1992).
[11] R. Bavli and H. Metiu, Phys. Rev. Lett. **69**, 1986 (1992); Phys. Rev. A **47**, 3299 (1993).
[12] M. Holthaus and D. Hone, Phys. Rev. B **47**, 6499 (1993).
[13] D. Farelly and J. A. Milligan, Phys. Rev. E **47**, R2225 (1993).
[14] M. Morillo and R. I. Cukier, J. Chem. Phys. **98**, 4548 (1993).

[15] R. I. Cukier and M. Morillo, Chem. Phys. **183**, 375 (1994).
[16] Yu. I. Dakhnovskii and R. Bavli, Phys. Rev. B **48**, 11 010 (1993); **48**, 11 020 (1993); Phys. Rev. A **48**, 1050 (1993); J. Phys. Chem. **98**, 9777 (1994).
[17] D. E. Makarov, Phys. Rev. E **48**, R4146 (1993).
[18] D. E. Makarov and N. Makri, Phys. Rev. B **52**, R2257 (1995).
[19] R. P. Feynman and F. L. Vernon, Ann. Phys. **24**, 118 (1963).
[20] D. E. Makarov and N. Makri, Chem. Phys. Lett. **221**, 482 (1994).
[21] N. Makri and D. E. Makarov, J. Chem. Phys. **102**, 4600 (1995).
[22] N. Makri and D. E. Makarov, J. Chem. Phys. **102**, 4611 (1995).
[23] N. Makri, E. Sim, D. E. Makarov, and M. Topaler (unpublished).
[24] N. Makri, Chem. Phys. Lett. **193**, 435 (1992); in *Time-Dependent Quantum Molecular Dynamics,* edited by J. Broeckhove and L. Lathowers (Plenum, New York, 1992), p. 203.
[25] M. Topaler and N. Makri, J. Chem. Phys. **97**, 9001 (1992); Chem. Phys. Lett. **210**, 285 (1993); **210**, 448 (1993).
[26] D. E. Makarov and N. Makri, Phys. Rev. A **48**, 3626 (1993).
[27] G. Ilk and N. Makri, J. Chem. Phys. **101**, 6708 (1994).
[28] N. Makri, J. Math. Phys. **36**, 2430 (1995).
[29] M. Topaler and N. Makri, J. Chem. Phys. **101**, 7500 (1994).
[30] A. O. Calderia and A. J. Leggett, Physica A **121**, 587 (1983).
[31] We use the term *tensor* as synonymous with multidimensional array or matrix and do not imply that these objects satisfy the transformation properties of tensors.
[32] J. H. Shirley, Phys. Rev. **138**, B979 (1965).
[33] J. Plata and J. M. Gomez Llorente, Phys. Rev. A **48**, 782 (1993).
[34] *Handbook of Mathematical Functions,* edited by M. Abramowitz and I. A. Stegun (Dover, New York, 1972).
[35] F. Grossmann, T. Dittrich, P. Jung, and P. Hänggi, J. Stat. Phys. **70**, 229 (1993).
[36] T. Dittrich, B. Oeschlägel, and P. Hänggi, Europhys. Lett. **22**, 5 (1993).
[37] A. Abragam, *Principles of Nuclear Magnetism* (Oxford University Press, New York, 1961).
[38] Yu. I. Dakhnovskii and R. D. Coalson, J. Chem. Phys. **103**, 2908 (1995).
[39] Yu. Dakhnovskii, Ann. Phys. (N.Y.) **230**, 145 (1994); Phys. Rev. B **49**, 4649 (1994).
[40] For a review, see P. Jung, Phys. Rep. **234**, 175 (1993), and the entire issue of J. Stat. Phys. **70**, Nos. 1 and 2 (1993).
[41] B. McNamara and K. Wiesenfeld, Phys. Rev. A **39**, 4854 (1989).
[42] R. Löfstedt and S. N. Coopersmith, Phys. Rev. Lett. **72**, 1947 (1994); Phys. Rev. E **49**, 4821 (1994).
[43] M. Grifoni, M. Sassetti, J. Stockburger, and U. Weiss, Phys. Rev. E **48**, 3497 (1993).
[44] M. Grifoni, M. Sassetti, P. Hänggi, and U. Weiss (unpublished).
[45] B. B. Laird, J. Budimir, and J. L. Skinner, J. Chem. Phys. **94**, 4391 (1991).
[46] E. Geva, R. Kosloff, and J. L. Skinner, J. Chem. Phys. **102**, 8541 (1995).
[47] H. Dekker, J. Phys. C **20**, 3643 (1987).
[48] S. Mukamel and K. Shan, Chem. Phys. Lett. **117**, 489 (1985).
[49] D. G. Evans, R. D. Coalson, H. Kim, and Y. Dakhnovskii, Phys. Rev. Lett. (to be published).